



Search for variable stars in the Carina dSph galaxy

A. Munteanu¹, M. Monelli^{2,3}, A. R. Walker⁴, G. Bono², P. B. Stetson⁵, R. Buonanno²,
F. Caputo², C. E. Corsi², M. Nonino⁶, L. Pulone², H. A. Smith⁷

¹ ICREA - Universitat Pompeu Fabra, Dr. Aiguader 80, 08003 Barcelona, Spain

² INAF - Osservatorio Astronomico di Roma, Via Frascati 33, 00040 Monte Porzio Catone, Italy

³ Instituto de Astrofísica de Canarias, C/ Via Lactea E-38205 La Laguna, Tenerife, Spain

⁴ CTIO, NOAO, Casilla 603, La Serena, Chile

⁵ Dominion Astrophys. Obs., Herzberg Institute of Astrophysics, 5071 West Saanich Road Victoria, BC V9E 2E7, Canada

⁶ Osservatorio Astronomico di Trieste, via Tiepolo 11, 40131 Trieste, Italy

⁷ Michigan State University, East Lansing, MI 48824, USA

Abstract. We discuss methods and preliminary results in a search for variable stars in the Carina dSph galaxy. This galaxy presents a complex star formation history and hosts a unique sample of variable stars. We collected B,V time series data during different runs, from 1999 to 2004, with the MOSAICII camera available at 4m CTIO telescope. The methodology is based on correlations between a version of the Welch-Stetson variability index, the variability probability of the Lomb-Scargle periodogram, and general statistical parameters associated with the individual light curves.

Key words. Galaxies: dwarf – Galaxies: individual (Carina) – Stars: variables – Methods: data analysis

1. Introduction

Among dwarf Spheroidal (dSph) galaxies, Carina is one of the most interesting objects, since its complex and recent star formation history is at odds with predictions based on recent cosmological simulations. The existence of multiple stellar populations at the same distance allows the simultaneous observation of variable stars with different ages and in different stages of stellar evolution. Old and intermediate-age variable stars during the

core He-burning phase (RR Lyrae, Anomalous Cepheids) and H-burning phase (Oscillating BSs, δ Scuti) have already been detected in the Carina dSph (Saha et al. 1986; Mateo et al. 1998). The present work is part of a long-term project aimed at studying both static and variable stars in Carina (Dall'Ora et al. 2003; Monelli et al. 2003). In particular, we are interested in improving the detection of variable stars using the B,V time series data collected during different runs, from 1999 to 2004, with the MOSAICII camera available at the 4m CTIO telescope (see Monelli et al. in this vol-

ume). Our work involved two main phases: improving the calibration technique and extracting correlations between several statistical variability indicators.

The photometric catalogue includes B,V time series for $\approx 10^5$ stars that range from a few measurements in the outermost regions to 54 inside the galaxy core. The current analysis only considers stars with more than ten measurements in both B and V bands.

2. Data Calibration

The color calibration was performed on each of the n measurements using calibration curves of the form: $M_i = m_i + A_m + C_m(\bar{b} - \bar{v})$, where $i = 1, n$ are the individual phase points, while $M = \{B, V\}$ and $m = \{b, v\}$ refer to Johnson and instrumental magnitudes, respectively. The instrumental magnitudes have been corrected for atmospheric extinction, aperture effects, and normalized to an exposure time of 1 sec. The overlined terms refer to the weighted mean of B,V instrumental magnitudes. However, such an approach might provide values far from the intrinsic mean magnitudes, due to either under-sampled asymmetric light curves or to a substantial difference in B,V amplitudes. To overcome this problem our final calibration curve for the B-band was: $B_i = b_i + A_b + C_b(b_i - \bar{v}_i)$, where \bar{v}_i refers to the weighted mean of the two V-band measurements which bridge in time the b_i measurement. The same approach was adopted for the V-band. The final photometric error has been propagated by accounting also for the error in the individual A_m, C_m constants.

3. Variability Indicators

For variability detection, we have used several direct and indirect indicators. As an obvious first step, we have determined the weighted mean (B, V), weighted variance (σ_B, σ_V) and weighted error ($\varepsilon_B, \varepsilon_V$) associated with each star. We also used a slightly different version of the normalized residual employed by Welch & Stetson (1993), defined here as:

$$\delta_B \equiv \sum_{i=1}^n \sqrt{\frac{n_B}{n_B - 1}} \frac{\varepsilon_B (B_i - B)}{\varepsilon_{B_i}}, \quad (1)$$

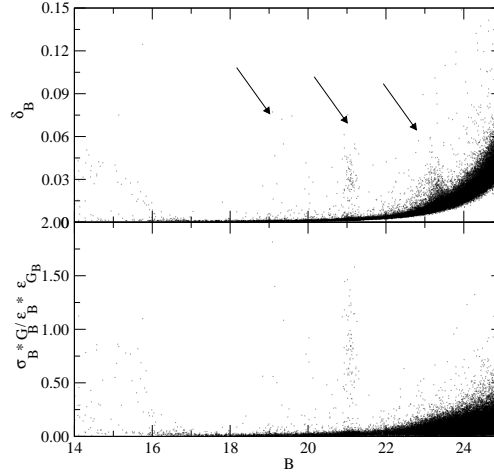


Fig. 1. *Top* - The variability index, δ_B , as a function of the B-band measurements. The three arrows mark from left to right the position of candidate Anomalous Cepheids ($B \approx 19 - 20$), RR Lyrae ($B \approx 21$), and δ Scuti ($B \approx 23.5$). *Bottom* - Same as the top, but for a nonlinear function of the variability indicators adopted to detect variable stars candidates. See §2 for more details.

for the B band, and an analogous definition for the V band data. Data plotted in the top panel of Fig. 1 show that this indicator is quite robust, and indeed different groups of candidate variable stars (Anomalous Cepheids, RR Lyrae, δ Scuti) can be easily identified. Additionally, we have used an indirect indicator introduced in Albrow & Gilliland (2001) for detecting eclipsing binaries and employed here with the more general aim of detecting significant departures from sinusoidal variation. It is defined as the ratio between the deviation of the mean value of the lowest five consecutive points from the total mean and the deviation of the mean value of the highest five consecutive points:

$$G_M \equiv \frac{M_{5min} - M}{M_{5max} - M}, \quad (2)$$

with M referring to either B or V band. We have chosen as selection criteria $G > 2$, as in Albrow & Gilliland (2001) and additionally $G/\varepsilon_G > 2$, where ε_G is the error associated with G .

We illustrate in Fig.1 the capability of the indicators to reveal potential variable stars. The candidates for variable stars are clearly visible above the general trend of the data and are indicated with arrows. The RR Lyrae or Anomalous Cepheids are better singled out by a nonlinear combination of the indicators (bottom panel). Owing to the low signal-to-noise ratio, the H-burning variables are more difficult to detect.

The most important direct variability indicator employed is the period determination using the Lomb-Scargle periodogram *weighted by the photometric errors of the individual points* (see Eqs. 1-3 from Woodward et al. 1994). This method performs a χ^2 sine-curve fit of unevenly spaced, unequally weighted data. For each trial frequency ω , the fit of the photometric measurements M_i has the form $f_i(t_i) = A \cos \omega(t_i - \tau) + B \sin \omega(t_i - \tau)$, where the constant τ is chosen to ease the χ^2 calculation by canceling the cross terms. The conditions leading to the best fit are (Cumming et al. 1999):

$$\sum w_i \sin \omega(t_i - \tau) \cos \omega(t_i - \tau) = 0 \quad (3)$$

$$\chi^2 = \sum w_i (M_i - f_i)^2; \quad \frac{\partial \chi^2}{\partial A} = \frac{\partial \chi^2}{\partial B} = 0, \quad (4)$$

with $w_i \equiv 1/\varepsilon_i^2$ being the weight of the point with photometric error ε_i . The normalized periodogram power is defined as

$$P_M(\omega) = \frac{n}{2\varepsilon_M^2 \sum w_i} \sum w_i f_i^2, \quad (5)$$

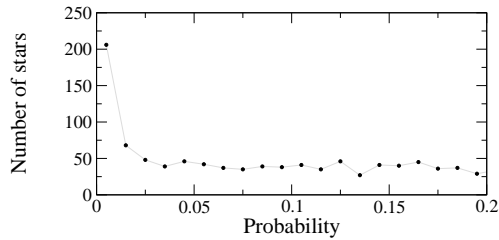


Fig. 2. A zoom of the histogram of the false-alarm probability of the highest peak associated to the B-band data for all stars: the increase in the number of stars towards low probabilities is produced by candidate variable stars.

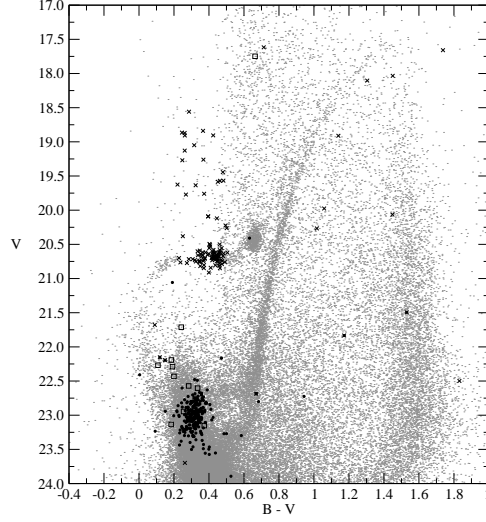


Fig. 3. Color-Magnitude Diagram of the entire sample of Carina stars. Crosses mark the identified variables, while squares the identified eclipsing binaries. Dots display candidate variable stars.

where M refers to either the B or the V-band measurements. Additionally, a false-alarm test is performed which provides probability that the highest periodogram peak is not a result of random, normally distributed noise. Therefore, a selection for low probability value of the Lomb-Scargle periodogram can be considered as an effective indicator of intrinsic variability (Fig. 2). More precisely, we have considered as candidate variable stars the objects presenting a peak probability in the range $[0, 0.1]$. We are aware that an aperiodic, non-Gaussian noise might produce a false periodogram peak. To overcome this thorny problem, we adopted a false-alarm test (Woodward et al. 1994; Albrow & Gilliland 2001), i.e. the same data have been randomly shuffled and for each extraction we estimated the periodogram.

4. Results and discussion

The selection process of candidate variable stars is based on a two-step method. In the first step, the candidates were selected on the basis of the values of their variability indicators. For example, we performed a polynomial

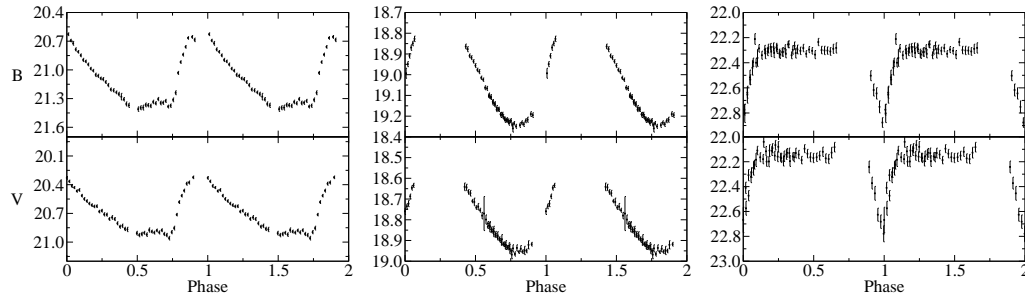


Fig. 4. A selection of identified variable stars: RR Lyrae – $P = 0.666$ days (left), Anomalous Cepheid – $P = 0.856$ days (middle), and eclipsing binary – $P = 0.5703$ days (right).

fit of all the data plotted in Fig. 1, and the stars located above one σ of this curve were selected as *bona fide* candidate variable stars. The union of all candidates selected using similar fits in both bands of all the variability indicators together with the candidates selected with the lowest false-alarm probability (Fig. 2) is our first sample of candidate variable stars. The second step implies a variability confirmation of these candidates through a visual examination of their light curves. Such an approach for the search for variable stars may appear clumsy when compared to other methods existent in the literature, such as Difference Image Photometry. The latter provides more accuracy for detecting variable stars, but not for identifying or classifying the detected variable stars. Therefore, we chose a method that allows us to search and classify the candidate variable stars.

The final list of candidates includes 145 identified variables (see Fig. 4) and 270 candidates still to be classified. The latter group includes stars whose estimated period is either not sufficiently accurate or for which the periods obtained using B and V-band data presents a large difference. The low signal-to-noise ratio and an apparently high irregularity of the light curve made classification difficult and also prompted us to improve our period estimation technique. However, these objects appear to be, by accounting for their position in the Color-Magnitude Diagram (dots in Fig. 3), either Oscillating Blue Stragglers or δ Scuti candidates. On the contrary, we have determined sufficiently accurate periods for the candidates we defined as “identified variables” (crosses in

Fig. 3). Among them, 79 are RR Lyrae stars and 19 are Anomalous Cepheids. Note that Dall’Ora et al. (2003) detected 75 RR Lyrae and 15 Anomalous Cepheids. For the remaining 34 objects we have not determined the exact variability type, but there is no doubt about their intrinsic variability, and thus we have included them in the category of identified variables.

Apart from these data, we also collected time series data with wide field imager available at the 2.2m ESO/MPI telescope (60 data points per band). Thus, one of the objectives of this project is the homogeneous relative and absolute zero-point calibration of all this data. Therefore, the final product of this work will include longer time series, more accurate and complete Color-Magnitude Diagram, as well as accurate pulsation properties for the identified variables.

Acknowledgements. A.M. acknowledges the INAF-OAR grants allowing her to conclude and present this work.

References

- Albrow, M. D. and Gilliland, R. L. 2001, ApJ, 559, 1060
- Cumming, A. et al. 1999, ApJ, 526, 890
- Dall’Ora, M. et al. 2003, AJ, 126, 197
- Mateo, M. et al. 1998, AJ, 115, 1856
- Monelli, M. et al. 2003, AJ, 126, 218
- Saha, A. et al. 1986, AJ, 322, L59
- Welch, D. L. and Stetson, P. B. 1993, AJ, 105, 1813
- Woodward, R. C. J et al. 1994, Icarus, 111, 45